

FATIGUE LIFE OF TWO STEELS UNDER COMBINED BENDING WITH TORSION – AN APPROACH INCLUDING NON-LOCAL STRAIN ENERGY DENSITY PARAMETER

Tadeusz Łagoda, Ewald Macha, Małgorzata Kohut
Henryk Achteлик, Aleksander Karolczuk, Adam Niesłony, Roland Pawliczek
Technical University of Opole,
ul. Mikołajczyka 5, 45-271 Opole, Poland
tlag@po.opole.pl, emac@po.opole.pl

Abstract

The paper contains the fatigue test results for 10HNAP and 18G2A steels under uniaxial constant-amplitude and random tension - compression as well as the test results for smooth and notched specimens of circular sections under proportional, non-proportional, constant-amplitude and random bending with torsion. Histories of the non-local equivalent strain energy density parameter in the critical plane were calculated. The paper contains a description of the applied procedure of fatigue life calculations under combined random bending and torsion, where cycles and half-cycles are counted according to the rain flow algorithm and damage is accumulated according to the Palmgren-Miner hypothesis. The calculated fatigue lives were compared with those obtained during experiments. A satisfactory efficiency of the proposed energy model of fatigue life calculations has been proved and its application for machine and structure elements where the stress gradients occur and subjected to multiaxial service loading has been presented.

Introduction

Experimental verification of the non-local parameter of strain energy density used in fatigue life calculations is the main aim of this paper. This verification was done for two steels: 10HNAP and 18G2A. The tests were performed under constant-amplitude, random proportional and non-proportional bending with torsion. Smooth and notched specimens were tested.

Experiments

Static properties of the tested materials are shown in Table 1 and their cyclic properties are presented in Table 2. Under constant-amplitude tension-compression, most of experimental results for the considered materials are included in the scatter bands with the coefficient equal to 3. Thus, if the fatigue life calculation results under multiaxial random loading are included in the same scatter band, the assumed model of fatigue life calculations can be accepted.

TABLE 1. Static properties of the tested materials

Material	R_e / MPa	R_m / MPa	A_{10} / %	Z / %	E / GPa	ν
10HNAP	414	566	32	60	215	0.29
18G2A	394	611	20	51	213	0.31

TABLE 2. Cyclic parameters of the tested materials

Material	σ'_f / MPa	b	m	σ_{af} / MPa	N_o / cycles
	Controlled strain		Controlled force		
10HNAP	1012	-0.11	9.82	252	1281000
18G2A	1190	-0.143	8.20	204	1240000

The fatigue tests under bending (B), combined bending with torsion (BT) and torsion (T) were performed on the fatigue test stands MZGS-100, MZGS-100L and MZGS-200L [2]. The tests under proportional constant-amplitude loading (smooth and notched specimens – Fig. 1) and random loading (B,BT,T) of 10HNAP and 18G2A steels were presented in [1]. This paper includes also tests results obtained under proportional constant-amplitude and non-proportional loading (BT), under proportional wide-band (B,BT,T) and narrow-band frequency random loading (B,BT) of 18G2A steel (smooth specimens). The fatigue tests of the smooth specimens were stopped when 10^7 cycles were obtained, the notched specimens were tested up to the moment when $5 \cdot 10^6$ cycles had been reached. Under random loading, tests of 10HNAP were stopped after 504000 seconds, and tests of 18G2A – after 330000 seconds. Undamaged specimens were assumed as having unlimited life.

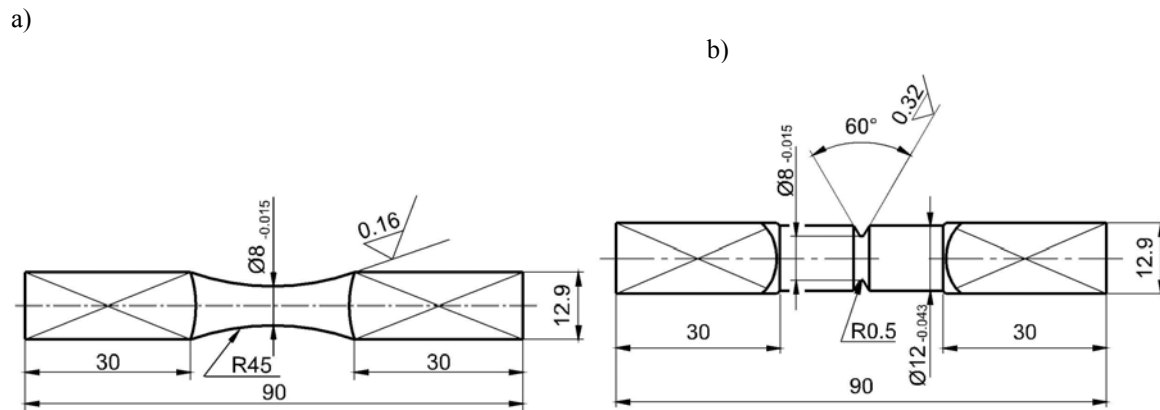


FIGURE 1. Geometrical forms of a) smooth and b) notched specimens subjected to fatigue tests

Algorithm for fatigue life determination

Fig. 2 shows a general algorithm for fatigue life determination under combined bending with torsion. The algorithm for fatigue life calculation according to the strain energy density parameter in the critical plane was partially verified in papers [2]. In this paper, the algorithm for combined bending with torsion including the non-local damage parameter is discussed. At stage 1, histories of the nominal normal stress $\sigma_{zz}(t)$ coming from bending and the nominal shear stress $\tau_{yz}(t)$ coming from torsion are registered. Next, stress distributions are determined in the cross-sections of smooth and notched specimens, assuming elastic behaviour of the material. Having the stress tensor histories, we determine elastic strain tensor components for the smooth specimen.

1	Recording of histories of nominal stresses coming from torsion and bending
2	Calculations of stress and strain distributions in the bar section
3	Determination of the critical plane position
4	Calculation of history of the equivalent parameter of strain energy density
5	Calculation of history of the non-local equivalent parameter of strain energy density
6	Counting of cycle and half-cycle amplitudes
7	Fatigue damage accumulation
8	Fatigue life determination

FIGURE 2. Algorithm for fatigue life determination

$$\varepsilon_{zz}^e(x, y, t) = \frac{\sigma_{zz}(x, y, t)}{E}, \quad (1)$$

$$\varepsilon_{yy}^e(x, y, t) = \varepsilon_{xx}^e(x, y, t) = -\nu \frac{\sigma_{zz}(x, y, t)}{E}, \quad (2)$$

$$\varepsilon_{yz}^e(x, y, t) = \frac{\tau_{yz}(x, y, t)}{2G}. \quad (3)$$

In the notched specimen, according to the Hooke's law, strains are determined from the following equations

$$\varepsilon_{xx}^e(x, y, t) = \frac{1}{E} \left[\sigma_{xx}(x, y, t) - \nu (\sigma_{zz}(x, y, t) + \sigma_{yy}(x, y, t)) \right], \quad (4)$$

$$\varepsilon_{yy}^e(x, y, t) = \frac{1}{E} \left[\sigma_{yy}(x, y, t) - \nu (\sigma_{xx}(x, y, t) + \sigma_{zz}(x, y, t)) \right], \quad (5)$$

$$\varepsilon_{zz}^e(x, y, t) = \frac{1}{E} \left[\sigma_{zz}(x, y, t) - \nu (\sigma_{xx}(x, y, t) + \sigma_{yy}(x, y, t)) \right], \quad (6)$$

and the strain $\varepsilon_{yz}^e(x, y, t)$ is determined according to Eq. (3), where stress distributions in the specimen section are modelled with the equations presented in [3].

The determined histories of the stress and strain tensors enable to calculate stress and strain histories in all directions $\bar{\eta}$ described by the direction cosines $\hat{l}_{\eta}, \hat{m}_{\eta}, \hat{n}_{\eta}$ related to the constant coordinate system $Oxyz$ connected with the specimen (stage 3). In this paper, the authors assumed the direction $\bar{\eta}$ which agrees with the direction \bar{z} and the direction \bar{s} which agrees with one of two remaining directions $\bar{\varphi}$, perpendicular to the direction $\bar{\eta}$.

According to the assumptions from the stage 4, the strain energy density parameter takes the following form

$$\begin{aligned} W_{eq}^e(x, y, t) &= \beta W_{z\varphi}^e(x, y, t) + W_{zz}^e(z, y, t) = \\ &= 0.5\beta\tau_{z\varphi}(x, y, t)\varepsilon_{z\varphi}^e(x, y, t)\text{sgn}[\tau_{z\varphi}(x, y, t), \varepsilon_{z\varphi}^e(x, y, t)] \\ &+ 0.5\sigma_{zz}(x, y, t)\varepsilon_{zz}^e(x, y, t)\text{sgn}[\sigma_{zz}(x, y, t), \varepsilon_{zz}^e(x, y, t)]. \end{aligned} \quad (7)$$

History of the strain energy density parameter $W_{eq}^e(x, y, t)$ – Eq. (7), presents changes of the parameter at time in the considered bar section. Assuming that $W_{eq}(x, y, t) = W_{eq}^e(x, y, t)$, we can determine history of the non-local equivalent parameter of strain energy density $\bar{W}_{eq}(t)$ (stage 5). At the next stage, histories of the non-local parameter of strain energy density $\bar{W}_{eq}(t)$ are schematized with the rain-flow algorithm and the counted cycles and half-cycles (stage 6) are used for damage accumulation (stage 7) according to the Palmgren-Miner hypothesis

$$S(T_o) = \begin{cases} \sum_{i=1}^j \frac{n_i}{N_o (W_{af}/\bar{W}_{ai})^{m'}} & \text{for } \bar{W}_{ai} \geq aW_{af} \\ 0 & \text{for } \bar{W}_{ai} < aW_{af} \end{cases}, \quad (8)$$

where $S(T_o)$ - damage degree at the observation time T_o , j – a number of classes in the amplitude histogram, W_{af} - fatigue limit expressed with the energy density parameter, $N_o - a$ number of cycles corresponding to the fatigue limit σ_{af} , n_i - a number of cycles with the amplitude \bar{W}_{ai} , $m' = m/2$ – exponent of the fatigue characteristics, $(W_a - N_f)$, a – coefficient allowing to include amplitudes of cycles below the fatigue limit in the fatigue damage accumulation.

After determination of the damage degree $S(T_o)$ from the non-local history $\bar{W}_{eq}(t)$, we determine the fatigue life (stage 8).

$$T_{cal} = \frac{T_o}{S(T_o)}. \quad (9)$$

Verification of the fatigue life calculation model

The discussed model of fatigue life was verified by comparison of the calculated results with the experimental ones. Some experimental results were verified in the previous papers. In [2] the calculation results are presented on similar graphs (Figs 3-7). The solid line expresses the perfect agreement between calculated and experimental results, the dashed lines show the scatter band with coefficient 3, characteristic for fatigue tests of steel specimens. In the case of smooth specimens, calculations were performed on the assumption that the fatigue life is influenced by energies of shear strains in two planes, i.e. $\beta = 2$:

$$\begin{aligned} W_{eq}(x, y, t) &= 2W_{z\varphi}^e(x, y, t) + W_{zz}^e(z, y, t) = \\ &= \tau_{z\varphi}(x, y, t)\varepsilon_{z\varphi}^e(x, y, t)\text{sgn}[\tau_{z\varphi}(x, y, t), \varepsilon_{z\varphi}^e(x, y, t)] \\ &+ 0.5\sigma_{zz}(x, y, t)\varepsilon_{zz}^e(x, y, t)\text{sgn}[\sigma_{zz}(x, y, t), \varepsilon_{zz}^e(x, y, t)]. \end{aligned} \quad (10)$$

For the notched specimens, the calculations were performed according to Eq. (10) assuming that the fatigue life is influenced by only one energy of shear strains ($\beta = 1$)

$$\begin{aligned} W_{eq}(x, y, t) &= W_{z\varphi}^e(x, y, t) + W_{zz}^e(z, y, t) = \\ &= 0.5\tau_{z\varphi}(x, y, t)\varepsilon_{z\varphi}^e(x, y, t)\text{sgn}[\tau_{z\varphi}(x, y, t), \varepsilon_{z\varphi}^e(x, y, t)] \\ &+ 0.5\sigma_{zz}(x, y, t)\varepsilon_{zz}^e(x, y, t)\text{sgn}[\sigma_{zz}(x, y, t), \varepsilon_{zz}^e(x, y, t)]. \end{aligned} \quad (11)$$

From Fig. 3 it appears that there is a good agreement between calculated and experimental fatigue lives for smooth specimens under proportional cyclic loading. Some very small departures can be observed for high lives near the fatigue limit and this is a typical fact in fatigue tests. A worse agreement was obtained for the specimens of 18G2A steel subjected to non-proportional loading (Fig. 4a). For the specimens of 10HNAP steel under random loading, quite a good agreement was obtained for the life close to $T_{exp}=10^5$ seconds (Fig. 4b). However, for less lives the calculation results are a little underrated, and for higher lives – overestimated. In tests of the specimens of 18G2A steel, a good agreement was obtained under wide-band frequency spectra (Fig. 5a) and a little overestimated results were obtained for narrow-band frequency spectra (Fig. 5b).

In the case of fatigue tests of notched specimens, calculations were made according to two directions for use. One of them included shear strain energy only in one plane (Fig. 6a for 10HNAP steel and Fig. 7a for 18G2A steel) – Eq. (11), and the second in two planes (Fig. 6b for 10HNAP and Fig. 7b for 18G2A) – Eq. (10). From the figures it appears that considering only one shear strain energy seems to be proper in the case of 18G2A steel. As for 10HNAP steel, the proposed calculation model seems to be very sensitive under pure torsion.

Conclusions

The procedure of fatigue life calculations under combined random bending with torsion includes some stages: determination of local strain and stress distributions in the bar section, determination of the critical plane position, determination of history of the equivalent strain energy density parameter, and next averaging the parameter in the critical plane on a part of the area in order to obtain history of the non-local parameter, schematization of random

history of the non-local parameter with the rain flow algorithm, damage accumulation according the Palmgren-Minera hypothesis and finally determination of the fatigue life.

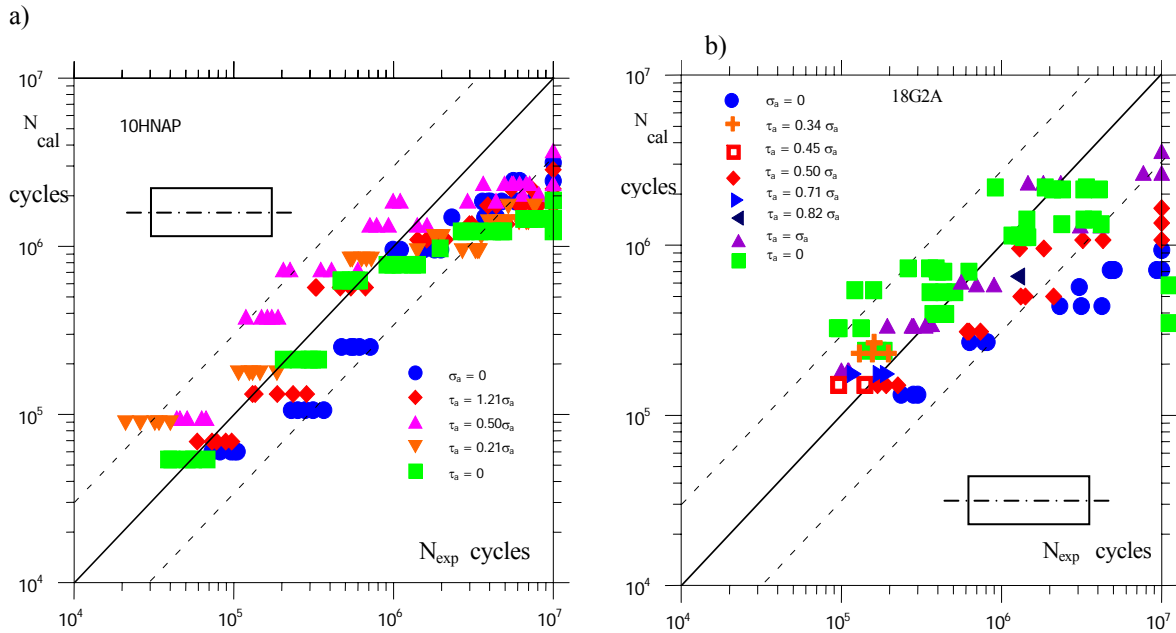


FIGURE 3. Comparison of calculated and experimental fatigue lives under constant-amplitude proportional bending with torsion for smooth specimens made of a) 10HNAP and b) 18G2A steels, according to Eq. (10)

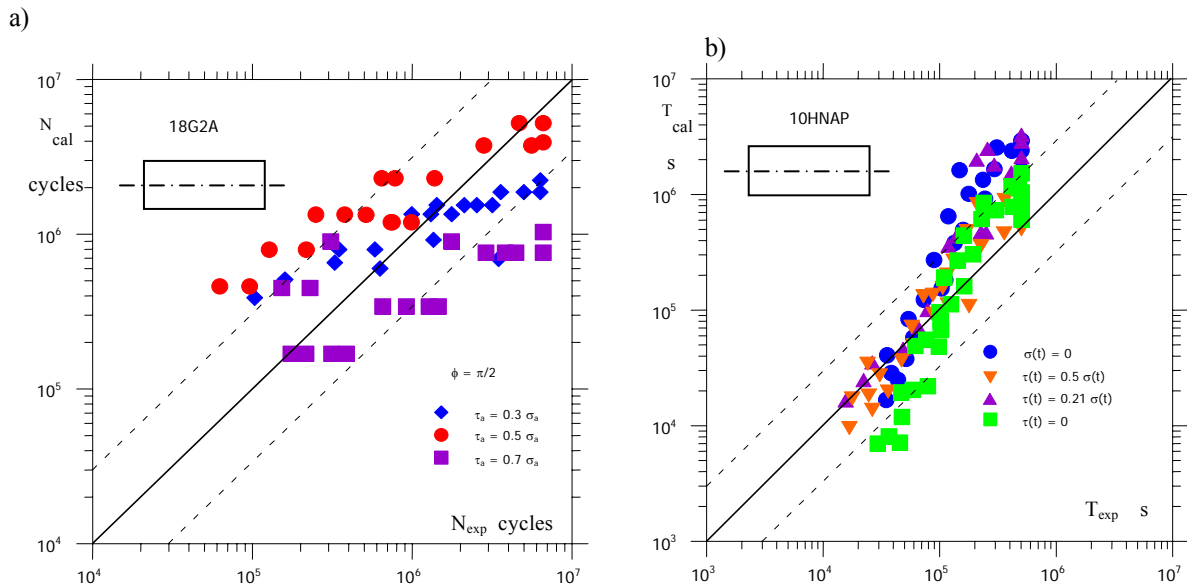


FIGURE 4. Comparison of calculated and experimental fatigue lives for smooth specimens made of a) 18G2A steel under constant-amplitude non-proportional bending with torsion and b) 10HNAP steel under random proportional bending with torsion, according to Eq. (10)

a)

b)

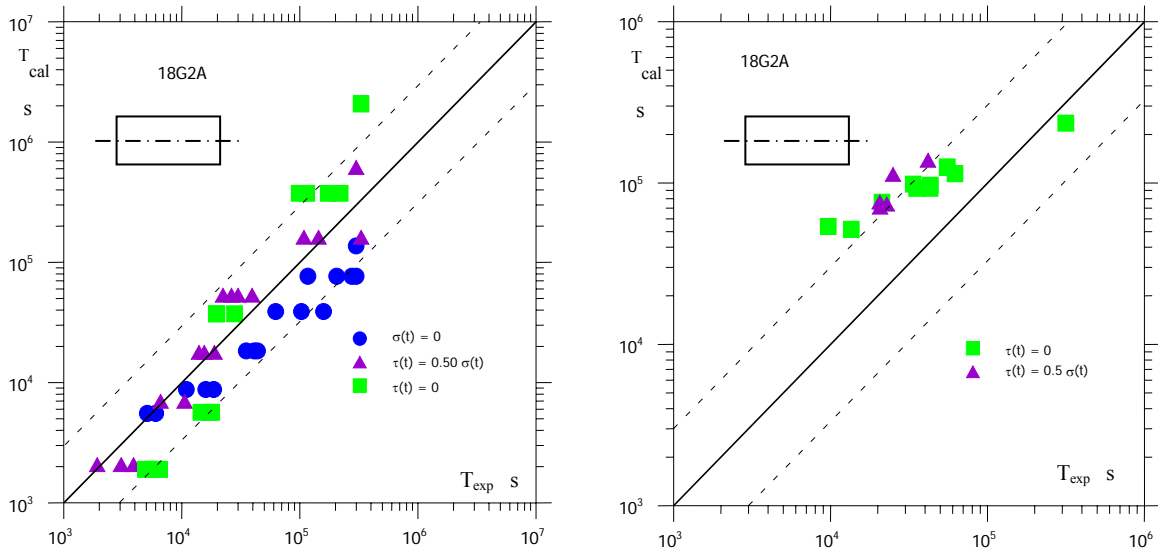


FIGURE 5. Comparison of calculated and experimental fatigue lives under random proportional bending with torsion for smooth specimens made of 18G2A steel a) with the wide-band and b) the narrow-band frequency spectrum, according to Eq. (10)

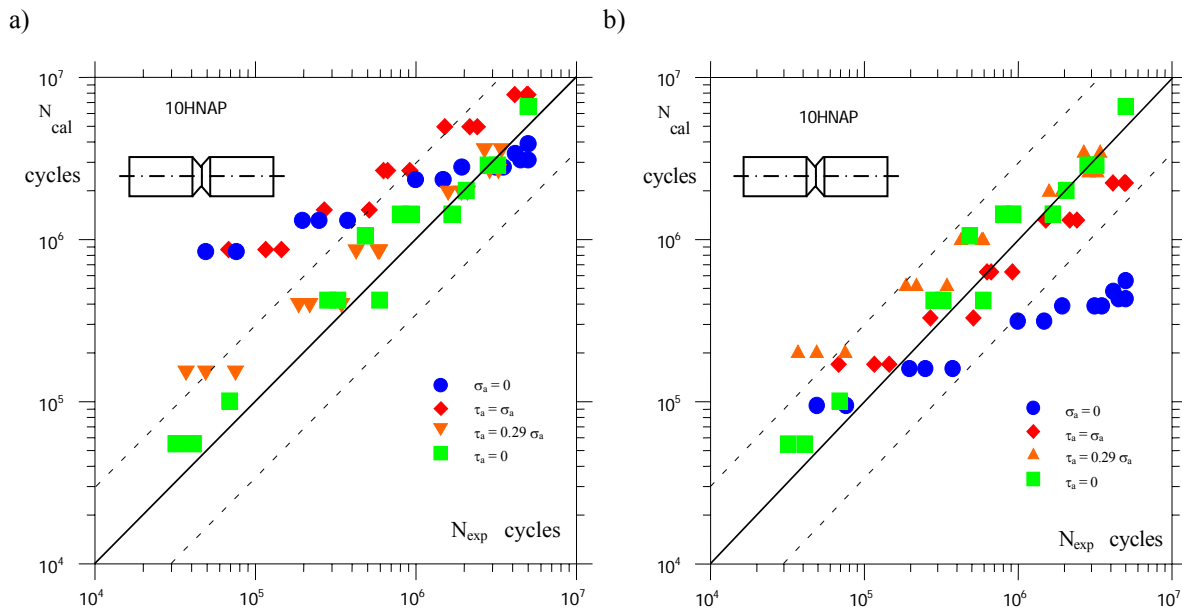


FIGURE 6. Comparison of calculated and experimental fatigue lives under cyclic proportional bending with torsion for notched specimens made of 10HNAP steel including shear strain energy a) only in one plane, according to Eq. (11) and b) in two planes, according to Eq. (10)

The non-local equivalent parameter of strain energy density is an averaged parameter in the critical plane area where the absolute value of the energy parameter history is greater than a certain level of energy expressed with the fatigue limit. For the tested steels: 10HNAP and 18G2A, the energy parameter including a half of the fatigue limit seems to be a proper level.

From the tests of smooth and notched specimens made of 10HNAP and 18G2A steels under proportional, non-proportional, constant-amplitude and random (with wide and narrow frequency bands) bending with torsion it results that the proposed energy models of fatigue

life calculations are efficient and they can be recommended for machine elements and structures with stress gradients.

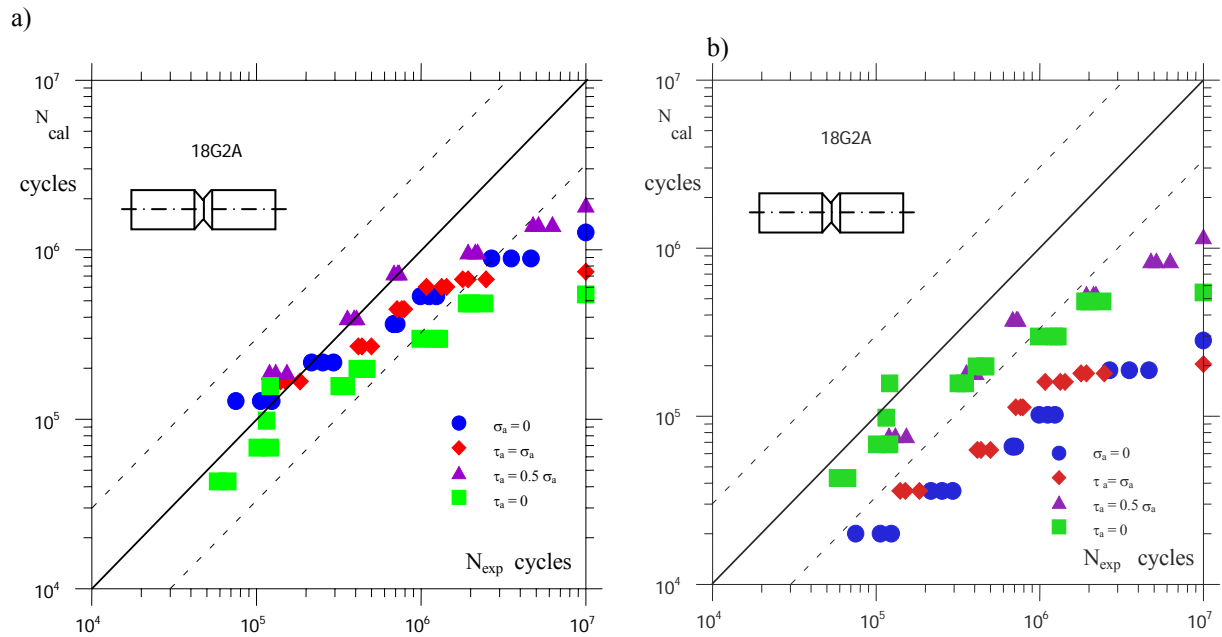


FIGURE 7. Comparison of calculated and experimental fatigue lives under cyclic proportional bending with torsion for notched specimens made of 18G2A steel with shear strain energy a) in one plane, according to Eq. (11) and b) in two planes, according to Eq. (10)

References

1. Łagoda, T., *Int. J. Fatigue*, vol.23, no 6, 467-480, 481-489, 2001.
2. Łagoda, T., Macha, E., Będkowski, W., *Int. J. Fatigue*, vol.21, 431-443, 1999.
3. Kohut, M., Łagoda, T., In: *Proceedings of the 15th European Conference on Fracture*, 2004.

With the support of the Commission of the European Communities under the FP5, GROWTH Programme, contract No. G1MA-CT-2002-04058 (CESTI).